

Ku70 stimulates fusion of dysfunctional telomeres yet protects chromosome ends from homologous recombination

Giulia B. Celli^{1,2,3}, Eros Lazzerini Denchi^{1,3} and Titia de Lange^{1,4}

Ku70–Ku80 heterodimers promote the non-homologous end-joining (NHEJ) of DNA breaks and, as shown here, the fusion of dysfunctional telomeres. Paradoxically, this heterodimer is also located at functional mammalian telomeres and interacts with components of shelterin, the protein complex that protects telomeres^{1–6}. To determine whether Ku contributes to telomere protection, we analysed *Ku70*^{-/-} mouse cells⁷. Telomeres of *Ku70*^{-/-} cells had a normal DNA structure and did not activate a DNA damage signal. However, Ku70 repressed exchanges between sister telomeres — a form of homologous recombination implicated in the alternative lengthening of telomeres (ALT) pathway⁸. Sister telomere exchanges occurred at approximately 15% of the chromosome ends when Ku70 and the telomeric protein TRF2 were absent. Combined deficiency of TRF2 and another NHEJ factor, DNA ligase IV, did not elicit this phenotype. Sister telomere exchanges were not elevated at telomeres with functional TRF2, indicating that TRF2 and Ku70 act in parallel to repress recombination. We conclude that mammalian chromosome ends are highly susceptible to homologous recombination, which can endanger cell viability if an unequal exchange generates a critically shortened telomere. Therefore, Ku- and TRF2-mediated repression of homologous recombination is an important aspect of telomere protection.

Although double-strand breaks (DSBs) activate the ATM kinase and are repaired by NHEJ and homologous recombination, the ends of chromosomes are not normally processed by these pathways. Cells make the distinction between DSBs and natural chromosome ends based on the telomeric complex, composed of TTAGGG repeats bound to shelterin (reviewed in ref. 9). Chromosome ends become a substrate for NHEJ when telomeres are damaged due to attrition of telomeric DNA or when the shelterin component TRF2 is inhibited. Deletion of TRF2 from *TRF2*^{fl/fl} mouse embryonic fibroblasts (MEFs), which contain an allele of *TRF2* that can be deleted with Cre–recombinase, results in the fusion of most telomeres, generating long trains of multiple joined chromosomes¹⁰ (Fig. 1a, b).

These fusions require DNA ligase IV (the ligase involved in NHEJ), indicating that the telomere fusions are formed by this pathway¹⁰. However, the role of Ku in telomere–telomere fusions had not been established and the presence of occasional telomere–telomere fusions in Ku-deficient cells^{2,4} argued against a strict requirement for Ku in the telomere fusion pathway.

To examine the role of Ku70 in telomere fusions, *TRF2*^{fl/fl} *Ku70*^{-/-} MEFs were generated and the deletion of TRF2 was induced with Cre. The G1–S arrest resulting from TRF2 loss¹¹ was circumvented by inactivating the p53 pathway, either genetically or with SV40 Large T antigen (SV40-LT). Deletion of *TRF2* in the *Ku70*^{-/-} cells was efficient and resulted in loss of TRF2 and its interacting partner Rap1 (see Supplementary Information, Fig. S1a, b and data not shown). NHEJ of the dysfunctional telomeres generated by *TRF2* deletion was reduced at least tenfold when *Ku70* was absent (Fig. 1a, b). Furthermore, genomic blots showed that the telomeric restriction fragments of *Ku70*^{-/-} cells persisted unaltered and retained their telomeric overhang (Fig. 1c and see Supplementary Information, Fig. S1d). We conclude that Ku70 is important for the removal of the telomeric overhang and the joining of telomeric ends after loss of TRF2. Whereas Ku70 deficiency lowered the frequency of telomere fusions by a factor 10, absence of DNA ligase IV reduced the telomere fusions by more than 100-fold¹⁰, suggesting that a subset of the telomere fusions require DNA ligase IV but not Ku. Ku-independent end joining has been described in *Saccharomyces cerevisiae*, where it was shown to utilize short regions of homology (micro-homology mediated end-joining, MMEJ¹²). It is possible that the two base pair (TA–AT) homology within each telomeric repeat is sufficient for Ku-independent MMEJ of mammalian telomeres.

End-loading of the Ku70–Ku80 ring-shaped complex onto DNA ends is thought to be an early step in NHEJ¹³. We propose that TRF2 blocks this step by hiding the telomere end in the t-loop structure. T-loops are an altered configuration of telomeres¹⁴, where the 3' telomeric overhang is paired with the duplex telomeric repeat array. It is not expected that the Ku70–Ku80 ring can load onto a chromosome end in the t-loop configuration. The requirement for TRF2 in repression of NHEJ is consistent

¹Laboratory for Cell Biology and Genetics, The Rockefeller University, 1230 York Avenue, New York, NY 10021, USA.

²Current address: Skirball Institute of Biomolecular Medicine, NYU School of Medicine, New York, NY. ³These authors contributed equally to this work.

⁴Correspondence should be addressed to T.L. (e-mail: delange@mail.rockefeller.edu)

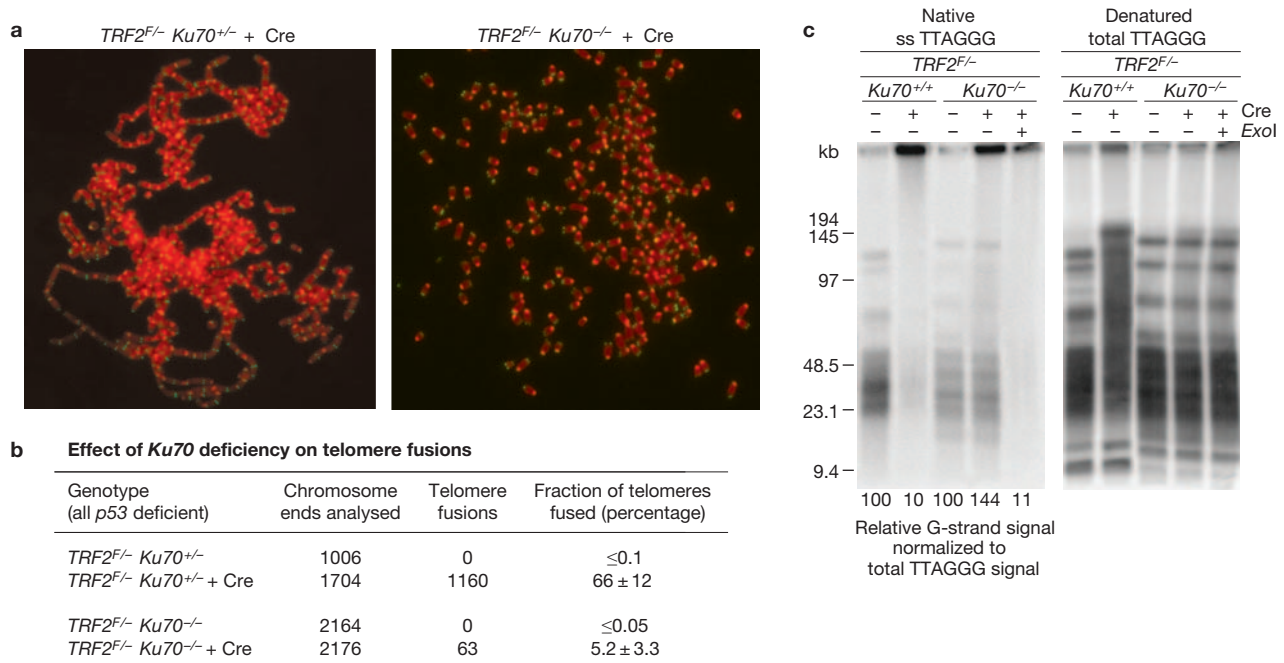


Figure 1 *Ku70* stimulates fusion of dysfunctional telomeres. **(a)** Metaphases from cells with the indicated genotypes 96 h after introduction of Cre. DNA stained with DAPI (false coloured in red). Telomeric DNA was detected by FISH (FITC, green). **(b)** Quantification of telomere fusion frequency in cells with the indicated genotypes. Telomere fusion frequencies were determined by inspection of images similar to those shown in **a** 96 h after introduction of Cre. **(c)** Genomic blot of telomeric restriction fragments of cells with the

with this model, as TRF2 has been implicated in t-loop formation in *in vitro* studies^{14,15}. Thus, TRF2-mediated t-loop formation may be a simple architectural mechanism by which functional telomeres block loading of *Ku70*–*Ku80* and thwart the NHEJ pathway.

Several observations have suggested that mammalian *Ku*, while promoting NHEJ of damaged telomeres, may protect chromosome ends. For example, mammalian *Ku* interacts with shelterin components *in vitro* and *in vivo*^{2,3,6} and can be detected at human telomeres by chromatin immunoprecipitation (ChIP)¹⁴. Furthermore, in unicellular eukaryotes and in plants, *Ku* has been shown to contribute to several aspects of telomere protection and telomere-length regulation^{16,17}. We therefore evaluated the contribution of *Ku70* to three aspects of telomere function: the maintenance of telomeric DNA; the repression of a DNA damage signal at chromosome ends; and the protection of telomeres from homologous recombination.

Ku70 deficiency did not lead to a significant change in the structure of the telomeric DNA or the ability of telomeres to avoid activation of a DNA damage signal at chromosome ends. Previous studies to assess the effect of *Ku* deficiency on telomere length resulted in conflicting reports^{4,18,19}. Our data showed no significant change in the length of the telomeric repeat array and, as reported previously¹⁹, the 3' telomeric overhang of *Ku70^{-/-}* MEFs was not significantly altered compared with wild-type *Ku70* littermate controls (Fig. 1c and see Supplementary Information, Fig. S1c). We next asked whether *Ku* is required to repress the activation of a DNA damage signal at chromosome ends. The accumulation of DNA damage response factors (such as γ -H2AX and 53BP1), in so called telomere dysfunction induced foci (TIFs) at chromosome ends is a well-established indicator of telomere dysfunction^{10,20,21}. *Ku70^{-/-}* cells showed no evidence of significant telomere deprotection based on the TIF assay (Fig. 2a–c).

indicated genotypes before and after introduction of Cre. DNA was harvested 96 hours after Cre expression, digested with *Mbo*I and hybridized with a telomere specific probe. In-gel hybridization to native DNA and rehybridization after *in situ* denaturation are shown. DNAs were treated with *Escherichia coli* exonuclease I as indicated. The single-stranded telomeric DNA signal was normalized to the total telomeric DNA signal in each lane. The numbers below the gel represent the ratios relative to the value obtained in the first lane.

Furthermore, *Ku70^{-/-}* cells did not show the high level of Chk2 phosphorylation observed in cells that experienced telomere deprotection on deletion of *TRF2* (Fig. 2d). The moderate level of Chk2 phosphorylation observed in *Ku70^{-/-}* and *Lig4^{-/-}* cells (Fig. 2d) is likely due to their NHEJ deficiency. Taken together, these data suggest that most of the telomeres in *Ku70^{-/-}* cells have a normal DNA structure and retain the ability to mask the chromosome ends from the DNA damage surveillance.

In contrast, *Ku70* contributes to the protection of telomeres from homologous recombination between sister telomeres (telomere sister-chromatid exchange, T-SCE^{22,23}). This process can shorten and elongate individual telomeres when the exchanged segments are not equal (Fig. 3a). T-SCEs can be monitored using chromosome-orientation fluorescent *in situ* hybridization (CO-FISH²⁴), which detects the parental TTAGGG and CCCTAA strands of the two sister telomeres at one end of metaphase chromosomes (Fig. 3a). The rate of T-SCE was not significantly increased in *Ku70^{-/-}* cells compared with *Ku70^{+/-}*, *Ku70^{+/+}* and *Lig4^{-/-}* cells (Fig. 3d, e and Table 1). In each setting, between 1.5–3% of the chromosome ends displayed evidence of a T-SCE event. Although this basal rate of sister chromatid exchanges is high compared with the rest of the genome, it is consistent with the data presented in other studies^{25,26}. T-SCEs were also not significantly elevated in absence of TRF2. This conclusion was based on conditional deletion of *TRF2* from *TRF2^{F/-}Lig4^{-/-}* cells, which do not undergo telomere fusion so that the fate of unligated telomere ends could be determined (Fig. 3e and Table 1).

Although loss of *Ku70* or TRF2 alone had no significant effect, absence of both proteins greatly increased the rate of T-SCEs. Approximately 15–20% of chromosome ends showed T-SCEs in *TRF2^{F/-}Ku70^{-/-}* cells treated with Cre (Fig. 3b, c and Table 1). The median frequency of T-SCEs showed a wide

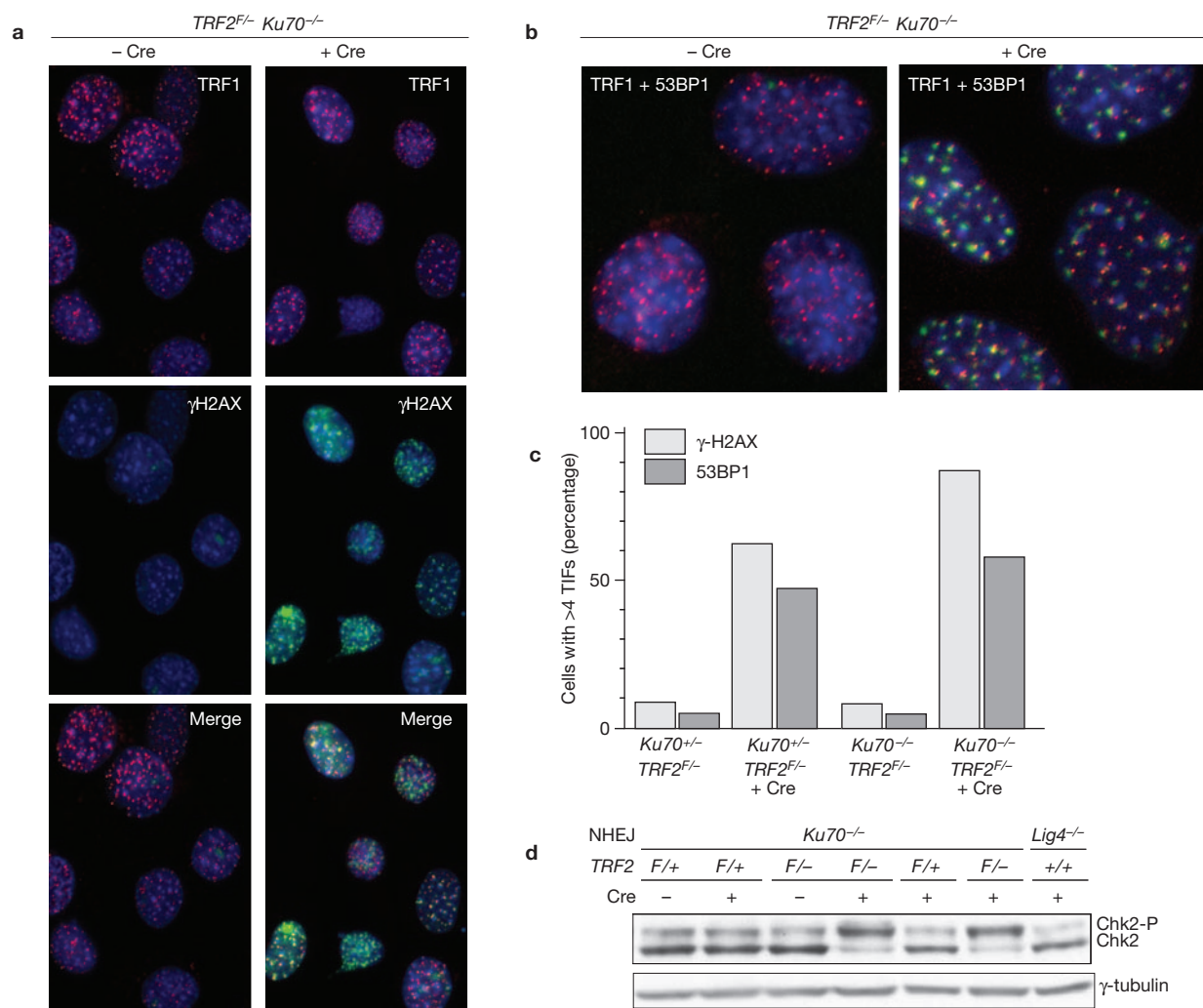


Figure 2 Absence of a significant telomere DNA damage signal in *Ku70^{-/-}* cells. **(a)** TIF analysis on *TRF2^{F/-} Ku70^{-/-}* cells before and after introduction of Cre. Immunofluorescence for γ -H2AX (Alexa488, green) and TRF1 (RRX, red), merged with DAPI stain for DNA (blue). **(b)** TIF analysis on *TRF2^{F/-} Ku70^{-/-}* cells after Cre. Immunofluorescence for 53BP1 (Alexa488, green) and TRF1 (RRX, red), merged with DAPI stain for DNA (blue). Cells were analysed 96 h after introduction of Cre. **(c)** Quantification of the percentage of TIF-positive cells versus the indicated *Ku70* and *TRF2* status. TIFs

range for individual metaphase cells (0–48%). There were no metaphases in which more than 50% of the chromosome ends showed T-SCEs. A maximum frequency of 50% is expected if homologous recombination generates crossover and non-crossover events in a one to one ratio. Metaphases in which almost 50% of the telomeres showed T-SCEs suggest that, in these cells, most telomeres participated in a recombination event during or after their replication. The observed T-SCE events showed various exchange ratios, ranging from near reciprocal to exchanges that were detectable with only one of the two probes (Fig. 3b, c). Such unequal exchanges are expected to alter the lengths of the sister telomeres (Fig. 3a).

In addition to T-SCEs, inappropriate homologous recombination at telomeres can have a second outcome — the deletion of t-loop-sized segments²⁷. Referred to as t-loop homologous recombination, these deletions are thought to involve the formation and resolution of a Holliday junction at the base of the t-loop. As is the case with T-SCEs, repression of t-loop homologous recombination involves TRF2. To determine whether the

were scored in >50 cells based on colocalization of γ -H2AX or 53BP1 with TRF1 as shown in **a** and **b**. Cells with >4 TIFs were scored as TIF positive. In *Ku70^{-/-} TRF2^{F/-}* cells treated with Cre most TIF positive cells contained >25 TIFs. Mean values derived from at least three experiments are given. **(d)** Phosphorylation of Chk2 in cells with the indicated genotypes, with or without Cre treatment. Immunoblot of protein extracts prepared 96 h after introduction of Cre probed for phospho-Chk2. γ -tubulin served as a loading control. All of the nuclei shown in **a** and **b** are 8–15 μ m in diameter.

t-loop homologous recombination and T-SCEs are repressed by the same pathway, we made use of an amino-terminal deletion mutant of TRF2, TRF2 ^{Δ B}, which lacks the ability to repress t-loop homologous recombination while retaining the ability to protect telomeres from NHEJ²⁷. To examine whether TRF2 ^{Δ B} was also deficient in repression of T-SCEs, *TRF2^{F/-} Ku70^{-/-}* and *TRF2^{F/-} Ku70^{+/-}* controls were infected with retroviral vectors encoding full-length TRF2 or TRF2 ^{Δ B} (see Supplementary Information, Fig. S1b, d). As expected, both TRF2 proteins repressed the telomere-fusion phenotype associated with TRF2 deficiency (see Supplementary Information, Fig. S1d and data not shown). In addition, full-length TRF2 and TRF2 ^{Δ B} repressed the T-SCEs in Cre treated *TRF2^{F/-} Ku70^{-/-}* cells (see Supplementary Information, Fig. S1e). The simplest interpretation of these results is that t-loop homologous recombination and T-SCEs are repressed through distinct pathways.

These data reveal that telomeres require protection from homologous recombination between sister telomeres. The frequency of T-SCE at

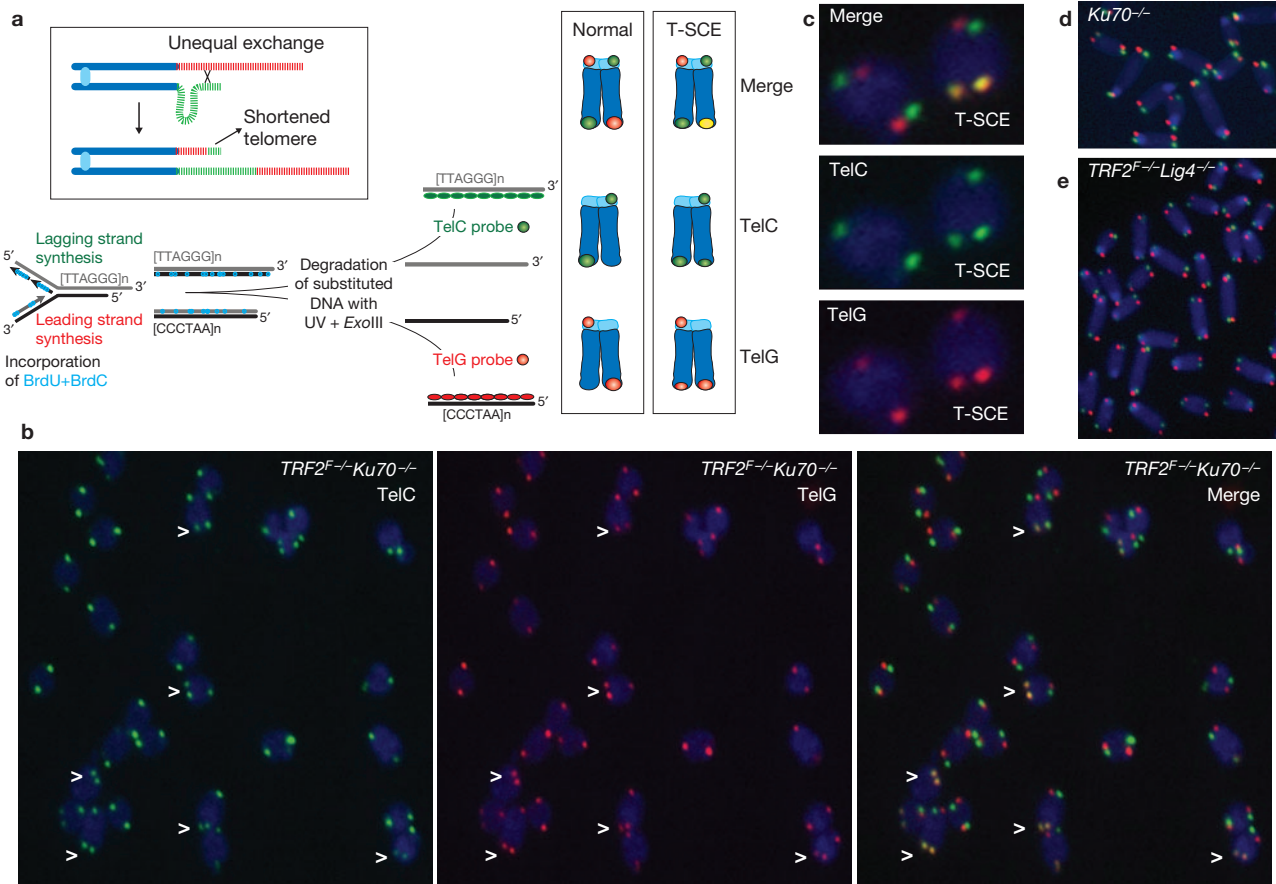


Figure 3 Induction of T-SCEs in absence of *TRF2* and *Ku70*. (a) Schematic representation of T-SCE detection using CO-FISH. The boxed inset shows a simplified schematic representation of telomere-length alterations through dysfunctional telomeres is remarkably high. Assuming an average size for mouse telomeres of approximately 30 kb and a median T-SCE rate of 15%, the rate of sister-chromatid exchanges in this part of the genome is 2–3 orders of magnitude higher than elsewhere. The propensity of unprotected telomeres to undergo homologous recombination may simply be due to fact that they are DNA ends. Protection requires either TRF2 or Ku70 (and by inference, Ku80). The finding that Ku represses T-SCEs at mammalian telomeres is consistent several observations: inhibition of homologous recombination at IScE1 and RAG-induced breaks^{28,29}; observations on DSB processing in *Ku*-deficient chicken DT-40 cells³⁰; the proposal that Ku creates a barrier to recombination at telomeres in budding yeast³¹; the repression of budding yeast telomere-rapid deletions

unequal sister chromatid exchange. (b, c) T-SCEs in *TRF2*^{-/-}*Ku70*^{-/-} cells after treatment with Cre. (d, e) Absence of T-SCEs in *Ku70*^{-/-} cells that have TRF2, and in *TRF2*^{-/-}*Lig4*^{-/-} cells after treatment with Cre.

by Ku³²; and the induction of subtelomeric rearrangements in *Ku*-deficient fission yeast³³. In each of these examples, it seems that Ku has the ability to inhibit some aspect of homologous recombination.

How Ku and TRF2 prevent T-SCEs is not known, but a model is suggested by their shared ability to bind to the telomere terminus. Ku70–Ku80 binds DNA ends, regardless of their sequence, and has been shown to bind to DNA ends with TTAGGG repeats *in vitro*, even when flanked by a 3' overhang³⁴. TRF2 is a double-stranded TTAGGG-repeat binding protein that can bind to its duplex site, regardless of the context. However, TRF2 preferentially binds to its site when it is present at the end of a DNA with a 3' telomeric overhang¹⁵. Furthermore, TRF2 contributes to the recruitment of the single-stranded DNA binding protein POT1

Table 1 Effect of *Ku70*, *Lig4* and *TRF2* deficiency on T-SCE frequency

Cells ^a	Gene(s) deficient	Chromosome ends analysed ^b	Frequency of T-SCE per end ^c
<i>TRF2</i> ^{-/-} <i>Ku70</i> ^{-/-}	–	2380	2.6 ± 1.5% (n = 3)
<i>TRF2</i> ^{-/-} <i>Ku70</i> ^{-/-}	<i>Ku70</i>	2912	1.6 ± 1.4% (n = 4) ^d
<i>TRF2</i> ^{-/-} <i>Ku70</i> ^{-/-} + Cre	<i>Ku70</i> + <i>TRF2</i>	3617	15.5 ± 8.4% (n = 4) ^d
<i>TRF2</i> ^{-/-} <i>Ku70</i> ^{-/-} + Cre	<i>Ku70</i> + <i>TRF2</i>	4180	20.8 ± 15% (n = 4)
<i>TRF2</i> ^{-/-} <i>Lig4</i> ^{-/-}	<i>Lig4</i>	1934	1.9 ± 3.2% (n = 3)
<i>TRF2</i> ^{-/-} <i>Lig4</i> ^{-/-} + Cre	<i>Lig4</i> + <i>TRF2</i>	4003	3.9 ± 2.4% (n = 4)

^aAll cells lacked functional p53. ^bTotal number of chromosome ends analysed in three or four independent experiments. Only chromosome ends with clearly distinguishable sister telomeres were analysed. Chromosome ends that were fused or closely associated were excluded from analysis. ^cT-SCE events were analysed as shown in Fig. 3. ^dThis set of experiments involved cells expressing SV40 large T antigen.

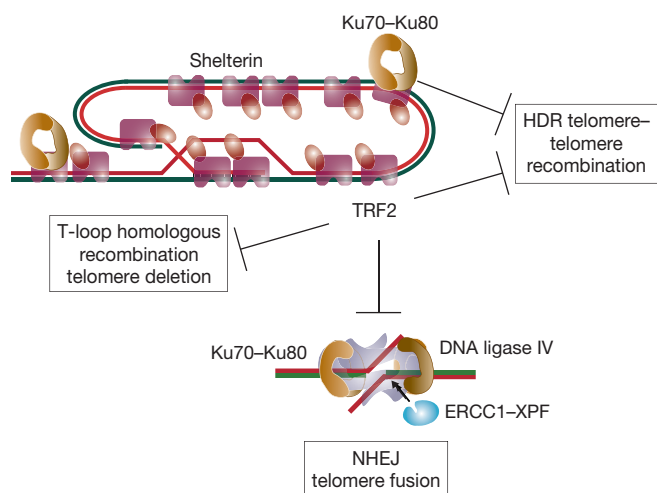


Figure 4 Schematic representation of the roles of TRF2 and Ku70 in repressing DSB repair at mammalian telomeres. TRF2 is required for the inhibition of NHEJ and concomitant overhang processing by the ERCC1–XPF nuclease. This function of TRF2 is proposed to depend on its ability to remodel telomeres into t-loops. Although protecting telomeres from NHEJ, t-loops are at risk of being deleted by homologous recombination if a Holliday junction is formed. TRF2 has a role in repressing t-loop homologous recombination through a function in its N-terminal basic domain. This report describes the role of TRF2 and Ku in repressing a third type of inappropriate repair at telomeres, recombination between sister telomeres. Thus, Ku threatens telomeres by mediating NHEJ, but also protects telomeres from homologous recombination.

to the telomere and the association of POT1 with the single-stranded overhang could further facilitate the positioning of TRF2–POT1 at the telomere terminus. Thus, both Ku70–Ku80 and TRF2 (with or without POT1) might be expected to associate with the chromosome end when telomeres occur in an ‘open’ state, for instance, during or immediately after DNA replication. The presence of Ku70–Ku80 or TRF2–POT1 at the telomere terminus may be sufficient to block the loading of homologous recombination factors.

Ku70–Ku80 is an important component of the NHEJ pathway and, as such, is a major contributor to the stability of mammalian chromosomes. The data presented here indicate that Ku70–Ku80 also functions in the maintenance of genome integrity through its protective role at telomeres. As Ku70–Ku80 acts in parallel with TRF2, its requirement for the repression of T-SCEs may not surface unless TRF2 is compromised. However, when telomeres become very short they contain less TRF2, therefore, the repression of T-SCEs by Ku70–Ku80 could become important for telomere stability. Consistent with this observation, T-SCEs are more frequent in late passage mouse telomerase RNA component null (*mTERC*^{-/-}) ES cells with very short telomeres²⁵. The repression of T-SCEs by Ku70–Ku80 could be particularly important in primary human somatic cells that undergo programmed telomere shortening. Increased T-SCEs at short telomeres could generate daughter cells with one or more dysfunctional telomeres (Fig. 3a). Interestingly, whereas Ku is not essential in the mouse, deletion of *Ku86* from human HTC116 cells results in a DNA damage signal and cell death after 8–10 cell doublings³⁵. As HTC116 cells have short telomeres, they may require Ku86 to repress T-SCEs and succumb to the lethal effects of critically shortened telomeres when *Ku86* is deleted. Our results also raise the possibility that the elevated T-SCE rate at the telomeres of human ALT cells⁸ is caused by a change in the Ku- and TRF2-mediated repression described here.

Collectively, the data suggest that mammalian telomeres use three distinct mechanisms to repress inappropriate DSB repair at chromosome ends (Fig. 4). TRF2 has a central role in each of these pathways by repressing NHEJ, intra-telomeric recombination (t-loop homologous recombination) and the telomere–telomere recombination detected by the T-SCE assay. It has been proposed that repression of NHEJ involves the formation of t-loops that could block end-loading of Ku (Fig. 4). Although the t-loop structure prevents NHEJ, it facilitates t-loop homologous recombination and this pathway is repressed by the basic N-terminal domain of TRF2 (ref. 27). The basic domain of TRF2 is not required to repress NHEJ or telomere–telomere recombination, indicating that repression of t-loop homologous recombination involves a distinct mechanism (Fig. 4). The repression of telomere–telomere recombination differs from the other two pathways in that it can be repressed by both Ku70 and TRF2. As our findings reveal that the type of DSB repair at natural chromosome ends can be directed by manipulating the status of Ku70 and TRF2, this system may be a valuable tool for studies of both telomere function and DSB repair in mammalian cells. □

METHODS

Conditional deletion of TRF2 from MEFs. TRF2 conditional knockout mice¹⁰ were crossed with *Ku70*^{-/-} mice⁷ (obtained from F. Alt, Harvard Medical School, Boston, MA) to generate E12.5–13.5 embryos. MEFs were generated according to standard protocols, immortalized at early passage ($\leq P2$) with pBabeSV40LT and infected with H&R Cre as described previously¹⁰.

Analysis of telomeric DNA by genomic blotting, FISH and CO-FISH.

Methods for CHEF gel electrophoresis of mouse telomeric DNA and FISH using a Tamra-[TTAGGG]₃ PNA probe (Applied Biosystems, Foster City, CA) were previously described¹⁰. DNA was counterstained with DAPI and slides were mounted in 90% glycerol, 10% PBS containing 1 $\mu\text{g ml}^{-1}$ p-phenylene diamine (Sigma, St Louis, MO). Images were captured with a Zeiss Axioplan II microscope and a Hamamatsu C4742-95 camera using Improvision OpenLab software. For CO-FISH, cells were grown in 10 μM BrdU:BrdC (3:1) for 16 h with the addition of 0.2 $\mu\text{g ml}^{-1}$ demecolcine for the final 2 h. Slides were treated with RNAase A (0.5 mg ml^{-1}) for 10 min at 37 °C, stained with Hoechst 33258 (0.5 $\mu\text{g ml}^{-1}$) in 2 \times SSC for 15 min at room temperature and exposed to 365-nm UV light (Stratalinker 1800 UV irradiator) for 30 min. Following digestion with Exonuclease III (10 U μl^{-1} ; Promega, Madison, WI) for 10 min at room temperature, slides were dehydrated through an ethanol series (70%, 95% and 100%) and incubated sequentially with TAMRA-TelG 5′-[TTAGGG]₃-3′ and FITC-TelC 5′-[CCCTAA]₃-3′ probes at room temperature. Control experiments were performed to ensure that the CO-FISH signals were dependent on the incorporation of BrdU/C and that the procedure did not generate signals due to unintended denaturation of the telomeric DNA.

Immunofluorescence microscopy and immunoblotting.

Immunofluorescence microscopy was performed as previously described¹⁰ using the following antibodies: TRF1, affinity purified rabbit peptide antibody against mTrf1 (644); TRF2, affinity purified rabbit antibody against GST–mTrf2 (1254); Rap1, affinity purified rabbit antibody against GST–mRap1 (1252); 53BP1, mouse monoclonal antibody 39 (a gift from T. Halazonetis, Wistar Institute, Philadelphia, PA); γ H2AX (Upstate Biotechnology, Lake Placid, NY). Secondary anti-mouse and anti-rabbit antibodies were labelled with Alexa 488 (MolecularProbes, Eugene, OR) and rhodamine red-X (RRX, Jackson ImmunoResearch, West Grove, PA), respectively. Immunoblots were prepared as previously described¹⁰ using antibody 1252 to mouse Rap1, antibodies to phospho-Chk2 (BD Bioscience, San Diego, Ca), antibodies to γ -tubulin (clone GTU 488; Sigma), or an anti-Myc antibodies (Ab 9E10). Blots were developed with enhanced chemiluminescence (ECL, Amersham, Piscataway, NJ).

Note: Supplementary Information is available on the Nature Cell Biology website.

ACKNOWLEDGEMENTS

We are grateful to F. Alt for providing the *Ku70* and *DNA ligase IV* knockout mice and to D. White for mouse husbandry. T. Halazonetis is thanked for generous gifts of the 53BP1 antibody. G.B.C. was supported by the Leukemia and Lymphoma Society. E.L.D. was supported by an Irma T. Hirsch fellowship. This work was supported by a grant from the National Institutes of Health (GM49046).

COMPETING FINANCIAL INTERESTS

The authors declare that they have no competing financial interests.

Published online at <http://www.nature.com/naturecellbiology/>

Reprints and permissions information is available online at <http://npg.nature.com/reprintsandpermissions/>

- Hsu, H. L., Gilley, D., Blackburn, E. H. & Chen, D. J. Ku is associated with the telomere in mammals. *Proc. Natl Acad. Sci. USA* **96**, 12454–12458 (1999).
- Hsu, H. L. *et al.* Ku acts in a unique way at the mammalian telomere to prevent end joining. *Genes Dev.* **14**, 2807–2812 (2000).
- Song, K., Jung, D., Jung, Y., Lee, S. G. & Lee, I. Interaction of human Ku70 with TRF2. *FEBS Lett.* **481**, 81–85 (2000).
- d'Adda di Fagagna, F. *et al.* Effects of DNA nonhomologous end-joining factors on telomere length and chromosomal stability in mammalian cells. *Curr. Biol.* **11**, 1192–1116 (2001).
- Gilley, D. *et al.* DNA-PKcs is critical for telomere capping. *Proc. Natl Acad. Sci. USA* **98**, 15084–15088 (2001).
- O'Connor, M. S., Safari, A., Liu, D., Qin, J. & Songyang, Z. The human Rap1 protein complex and modulation of telomere length. *J. Biol. Chem.* **279**, 28585–28591 (2004).
- Gu, Y. *et al.* Growth retardation and leaky SCID phenotype of Ku70-deficient mice. *Immunity* **7**, 653–665 (1997).
- Dunham, M. A., Neumann, A. A., Fasching, C. L. & Reddel, R. R. Telomere maintenance by recombination in human cells. *Nature Genet.* **26**, 447–450 (2000).
- de Lange, T. Shelterin: the protein complex that shapes and safeguards human telomeres. *Genes Dev.* **19**, 2100–2110 (2005).
- Celli, G. & de Lange, T. DNA processing not required for ATM-mediated telomere damage response after TRF2 deletion. *Nature Cell Biol.* **7**, 712–718 (2005).
- Smogorzewska, A. & de Lange, T. Different telomere damage signaling pathways in human and mouse cells. *EMBO J.* **21**, 4338–4348 (2002).
- Ma, J. L., Kim, E. M., Haber, J. E. & Lee, S. E. Yeast Mre11 and Rad1 proteins define a Ku-independent mechanism to repair double-strand breaks lacking overlapping end sequences. *Mol. Cell. Biol.* **23**, 8820–8828 (2003).
- Walker, J. R., Corpina, R. A. & Goldberg, J. Structure of the Ku heterodimer bound to DNA and its implications for double-strand break repair. *Nature* **412**, 607–614 (2001).
- Griffith, J. D. *et al.* Mammalian telomeres end in a large duplex loop. *Cell* **97**, 503–514 (1999).
- Stansel, R. M., de Lange, T. & Griffith, J. D. T-loop assembly *in vitro* involves binding of TRF2 near the 3' telomeric overhang. *EMBO J.* **20**, 5532–5540 (2001).
- Bertuch, A. A. & Lundblad, V. Which end: dissecting Ku's function at telomeres and double-strand breaks. *Genes Dev.* **17**, 2347–2350 (2003).
- Riha, K., Watson, J. M., Parkey, J. & Shippen, D. E. Telomere length deregulation and enhanced sensitivity to genotoxic stress in *Arabidopsis* mutants deficient in Ku70. *EMBO J.* **21**, 2819–2826 (2002).
- Espejel, S. *et al.* Mammalian Ku86 mediates chromosomal fusions and apoptosis caused by critically short telomeres. *EMBO J.* **21**, 2207–2219 (2002).
- Samper, E., Goytisolo, F. A., Slijepcevic, P., van Buul, P. P. & Blasco, M. A. Mammalian Ku86 protein prevents telomeric fusions independently of the length of TTAGGG repeats and the G-strand overhang. *EMBO Rep.* **1**, 244–252 (2000).
- d'Adda di Fagagna, F. *et al.* A DNA damage checkpoint response in telomere-initiated senescence. *Nature* **426**, 194–198 (2003).
- Takai, H., Smogorzewska, A. & de Lange, T. DNA damage foci at dysfunctional telomeres. *Curr. Biol.* **13**, 1549–1556 (2003).
- Bailey, S. M., Brenneman, M. A. & Goodwin, E. H. Frequent recombination in telomeric DNA may extend the proliferative life of telomerase-negative cells. *Nucleic Acids Res.* **32**, 3743–3751 (2004).
- Bechter, O. E., Zou, Y., Walker, W., Wright, W. E. & Shay, J. W. Telomeric recombination in mismatch repair deficient human colon cancer cells after telomerase inhibition. *Cancer Res.* **64**, 3444–3451 (2004).
- Bailey, S. M., Cornforth, M. N., Kurimasa, A., Chen, D. J. & Goodwin, E. H. Strand-specific postreplicative processing of mammalian telomeres. *Science* **293**, 2462–2465 (2001).
- Wang, Y. *et al.* An increase in telomere sister chromatid exchange in murine embryonic stem cells possessing critically shortened telomeres. *Proc. Natl Acad. Sci. USA* **102**, 10256–10260 (2005).
- Laud, P. R. *et al.* Elevated telomere-telomere recombination in WRN-deficient, telomere dysfunctional cells promotes escape from senescence and engagement of the ALT pathway. *Genes Dev.* **19**, 2560–2570 (2005).
- Wang, R. C., Smogorzewska, A. & de Lange, T. Homologous recombination generates T-loop-sized deletions at human telomeres. *Cell* **119**, 355–368 (2004).
- Pierce, A. J., Hu, P., Han, M., Ellis, N. & Jasin, M. Ku DNA end-binding protein modulates homologous repair of double-strand breaks in mammalian cells. *Genes Dev.* **15**, 3237–3242 (2001).
- Weinstock, D. M. & Jasin, M. Alternative pathways for the repair of RAG-induced DNA breaks. *Mol. Cell. Biol.* **26**, 131–139 (2006).
- Adachi, N., Ishino, T., Ishii, Y., Takeda, S. & Koyama, H. DNA ligase IV-deficient cells are more resistant to ionizing radiation in the absence of Ku70: Implications for DNA double-strand break repair. *Proc. Natl Acad. Sci. USA* **98**, 12109–12113 (2001).
- DuBois, M. L., Haimberger, Z. W., McIntosh, M. W. & Gottschling, D. E. A quantitative assay for telomere protection in *Saccharomyces cerevisiae*. *Genetics* **161**, 995–1013 (2002).
- Polotnianka, R. M., Li, J. & Lustig, A. J. The yeast Ku heterodimer is essential for protection of the telomere against nucleolytic and recombinational activities. *Curr. Biol.* **8**, 831–834 (1998).
- Baumann, P. & Cech, T. R. Protection of telomeres by the Ku protein in fission yeast. *Mol. Biol. Cell* **11**, 3265–3275 (2000).
- Bianchi, A. & de Lange, T. Ku binds telomeric DNA *in vitro*. *J. Biol. Chem.* **274**, 21223–21227 (1999).
- Li, G., Nelsen, C. & Hendrickson, E. A. Ku86 is essential in human somatic cells. *Proc. Natl Acad. Sci. USA* **99**, 832–837 (2002).

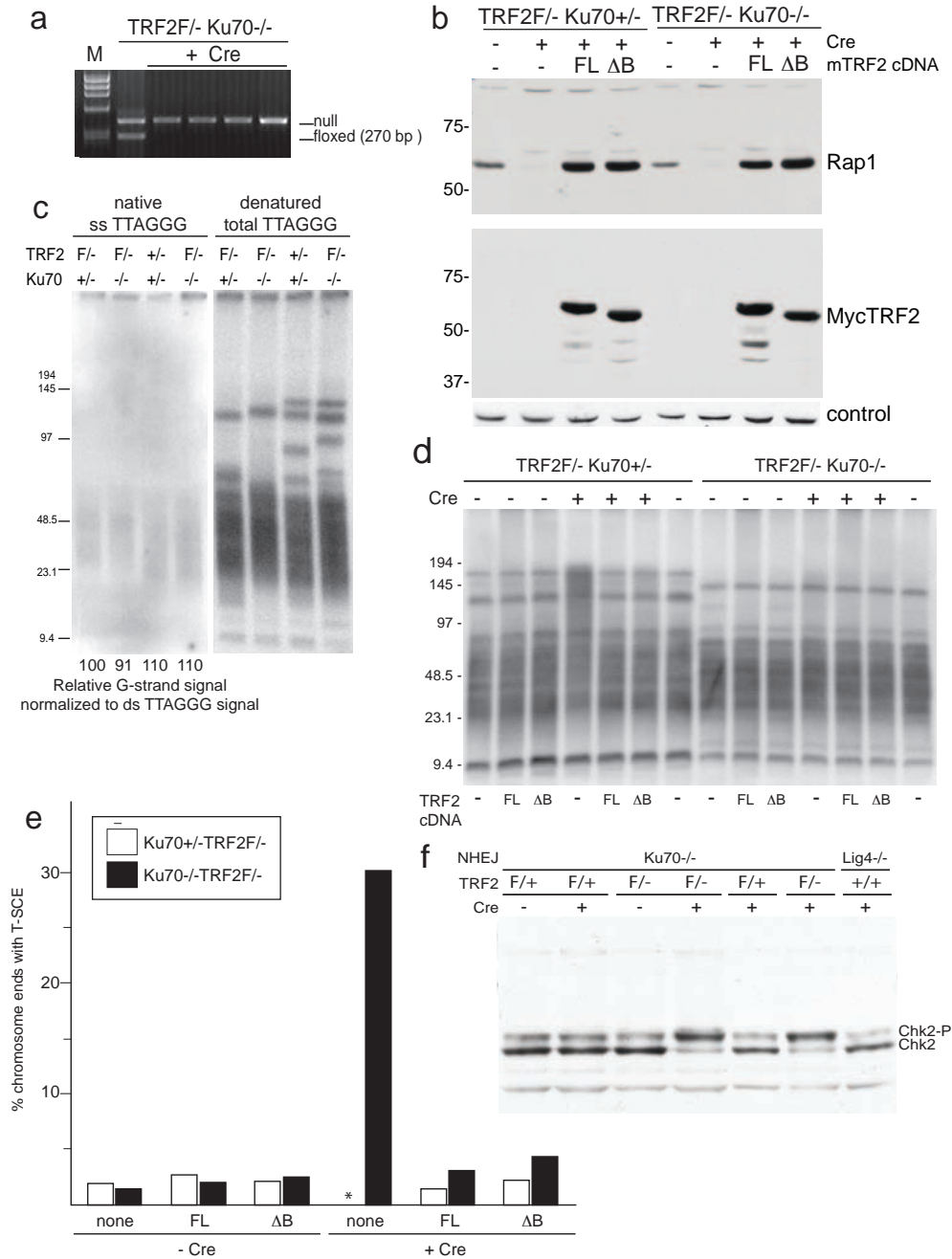


Figure S1 Cre-mediated deletion of TRF2 from TRF2F/-Ku70-/- cells, analysis of telomere status in Ku70-/- and Ku70+/- littermates, and suppression of T-SCEs by TRF2 and TRF2 Δ B. **(a)** PCR analysis of DNAs from cells with the indicated genotypes before or at 96 hours after introduction of Cre. **(b)** TRF2 deletion induces the expected loss of Rap1 protein and this effect is repressed by full length TRF2 and TRF2 Δ B. Immunoblot for TRF2 and Rap1 in cells with the indicated genotypes before and after deletion of TRF2 with Cre. Cell extracts were probed with an antibody to Rap1 (1252). TRF2 expression is detected with an antibody to the myc tag on these cDNAs (Ab 9E10). The loading control is a non-specific band in the Rap1 blot. **(c)** Ku70 deficiency does not lead to a significant change in telomere structure. CHEF gel of DNAs from four littermates with the indicated genotypes. Processing and quantification as in Fig. 1C. **(d)** Repression of telomere fusions induced by TRF2 deletion by full length TRF2 and TRF2 Δ B.

CHEF gel of DNAs from cells with the indicated genotypes treated with Cre as indicated. Cells carried retrovirally expressed alleles of TRF2 (FL, myc tagged full length TRF2; Δ B, myc tagged TRF2 Δ B). Telomere fusions result in increased MW of the telomeric fragments. **(e)** Repression of T-SCEs induced by TRF2 deletion by full length TRF2 and TRF2 Δ B. Cells with the indicated genotypes were infected with retrovirally expressed myc tagged TRF2, TRF2 Δ B, or the empty vector (none). Expression of the proteins is shown in panel b. Cells were treated with or without Cre and processed for T-SCE analysis as described in Figure 3. Bars indicate the frequency of T-SCE per chromosome end based on examination of 800 chromosome ends. A second independent experiment (not shown) showed similar repression of T-SCEs by full length TRF2 and TRF2 Δ B. The asterisk indicates that T-SCEs were not scored in TRF2F/-Ku70+/-p53-/- cells treated with Cre. These cells have prominent telomere-telomere fusions prohibiting evaluation of T-SCEs.